ISSN 1063-7826, Semiconductors, 2024, Vol. 58, No. 3, pp. 214–221. © Pleiades Publishing, Ltd., 2024.
Russian Text © The Author(s), 2023, published in Fizika i Tekhnika Poluprovodnikov, 2023, Vol. 57, No. 7, pp. 577–583.
English Text © Ioffe Institute, 2023.

Two-Subband Magnetotransport in GaAs Single Quantum Well with Superlattice Doping

A. A. Bykov[a], D. V. Nomokonov[a,*], I. S. Strygin[a], I. V. Marchishin[a], and A. K. Bakarov[a]

[a] *Rzhanov Institute of Semiconductor Physics, Siberian Branch, Russian Academy of Sciences, Novosibirsk, 630090 Russia*

**e-mail: nomokonov@isp.nsc.ru*

Received August 22, 2023; revised October 2, 2023; accepted October 2, 2023

Abstract—Two-subband magnetotransport of quasi-2D electron gas in GaAs single quantum well with AlAs/GaAs superlattice doping has been studied at $T = 4.2$ K in magnetic fields $B < 2T$. It was demonstrated that application of negative gate voltage leads to transformation of studied two-subband electron system into the one-subband system. This transformation is accompanied by appearance of positive magnetoresistance. This behavior has been described by conventional model of classical positive magnetoresistance that takes into account elastic intersubband scattering of electrons. Combined analysis of classical positive magnetoresistance and quantum magneto-intersubband oscillations makes it possible to define the values of transport rates of intrasubband scattering and quantum rate of intersubband scattering.

Keywords: quasi-twodimensional electron gas, positive magnetoresistance, two-subband system, magnetointersubband oscillations

DOI: 10.1134/S1063782624030047

1. INTRODUCTION

Two-subband magnetotransport of electrons in GaAs quantum wells with modulated doping has been investigated experimentally for more than 40 years [1]. At the initial stage of these studies, it was found that the filling of the second subband of dimensional quantization in the GaAs quantum well leads not only to the appearance of the second series of Shubnikov-de Haas (SdH) oscillations, but also to a decrease in the mobility (μ_0) of the quasi-two-dimensional electron gas [2]. In addition, GaAs quantum wells with two filled subbands of dimensional quantization E_1 and E_2, were found to exhibit classical positive magnetoresistance (PMR) due to the difference of mobilities in the subbands [3, 4]. It has also been shown that a new type of quantum resistance oscillations—magneto-intersubband (MIS) oscillations [5, 6] arises in two-subband electron systems.

The decrease of mobility μ_0 in a single GaAs quantum well when the second subband is filled, as well as the occurrence of MIS oscillations, confirmed the fundamental role of intersubband scattering in two-subband classical and quantum magnetotransport [7, 8]. Studies of two-subband magnetotransport in double GaAs-quantum wells have also confirmed the necessity to take into account intersubband scattering when interpreting classical PMR in bilayer electron systems [9–11], but the question of the contribution of intersubband scattering to classical PMR in single-layer systems is still open. In the present work, magnetotransport has been investigated in a single-layer two-subband electron system realized on the basis of a selectively doped single GaAs quantum well with short-period AlAs/GaAs superlattice barriers [12–15]. It is found that in such structures, as in double GaAs-quantum wells, the contribution of intersubband electron scattering to the classical PMR cannot be neglected. The obtained experimental data are analyzed within the framework of known theoretical models of classical and quantum transport in two-subband electron systems.

2. MAGNETORESISTANCE OF TWO-DIMENSIONAL SYSTEMS WITH TWO FILLED SUBBANDS

At low temperatures, when the electron gas is degenerate and elastic scattering on impurities or other inhomogeneities is the main scattering mechanism, the classical PMR in a two-subband system is expressed by the relation [9, 11]

$$\frac{\rho_{CPMR}}{\rho_0} = \frac{\omega_c^2 \nu_s/\nu_0 + \nu_r^2}{\omega_c^2 + \nu_r^2}, \quad (1)$$

where $\rho_0 = m\nu_0/e^2 n_s$—resistance in the zero magnetic field, $n_s = n_1 + n_2$, n_1 and n_2—electron densities in the subbands, $\omega_c = eB/m$—cyclotron frequency, B—external magnetic field, m—electron effective mass. The classical resistance increases with increasing B, start-

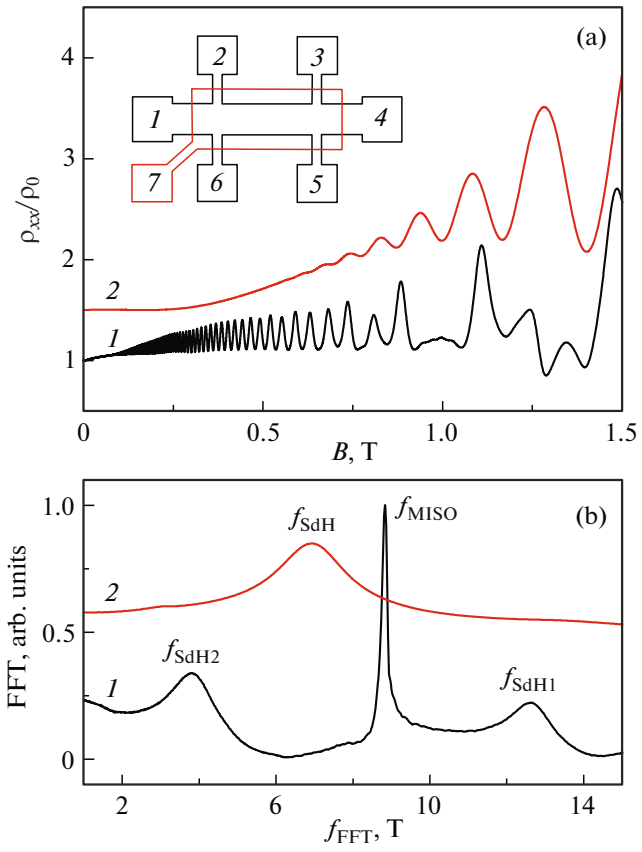

Fig. 1. (a) experimental dependencies of ρ_{xx}/ρ_0 on B: *1* — $V_g = 0$, *2*—$V_g = -2$ V. The inset shows a Hall bridge: *1–6*—ohmic contacts, *7*—Schottky field gate. (b) Fourier spectra of the dependencies of ρ_{xx}/ρ_0 on $1/B$: *1*—$V_g = 0$, *2*—$V_g = -2$ V. The curves *2* are shifted upwards for clarity. (The colored version of the figure is available on-line.)

ing at a value ρ_0, and reaches saturation at $\omega_c \gg \nu_r$. The characteristic relaxation rates ν_s, ν_r and ν_0 are given by the following expressions:

$$\nu_s = (n_1/n_s)\nu_{11}^t + (n_2/n_s)\nu_{22}^t + \nu_{12}^t, \quad (2)$$

$$\nu_r = (n_2/n_s)\nu_{11}^t + (n_1/n_s)\nu_{22}^t + 2\nu_{12}^q - \nu_{12}^t, \quad (3)$$

$$\nu_0 = (\nu_{11}^t + \nu_{12}^q)(\nu_{22}^t + \nu_{12}^q)/\nu_r - (\nu_{12}^q + \nu_{12}^t)^2 n_s^2/4n_1n_2\nu_r, \quad (4)$$

where ν_{11}^t and ν_{22}^t—transport relaxation rates in the first and second ($j = 1$ and 2) subbands E_j, and ν_{12}^t and ν_{12}^q—transport and quantum (single-particle) relaxation rates at intersubband scattering.

It is convenient to transform the system of equations (2)–(4) to the form where in the left-hand side are the unknown quantities ν_{11}^t, ν_{22}^t, ν_{12}^t and ν_{12}^q, and in the right-hand side—the characteristic relaxation rates ν_0, ν_s and ν_r known from experiment:

$$\nu_{12}^q - \nu_{12}^t = 2(n_1n_2/n_s^2)(\nu_r - \nu_s) \pm (n_1/n_s - n_2/n_s)R, \quad (5)$$

$$\nu_{11}^t + \nu_{12}^t = (n_1/n_s)(1 + 2n_2/n_s)\nu_s - (n_2/n_s^2)(n_1 - n_2)\nu_r \pm 2(n_2/n_s)R, \quad (6)$$

$$\nu_{22}^t + \nu_{12}^t = (n_2/n_s)(1 + 2n_2/n_s)\nu_s + (n_1/n_s^2)(n_1 - n_2)\nu_r \mp 2(n_1/n_s)R, \quad (7)$$

where $R \equiv (2/n_s)[\nu_r(\nu_s - \nu_0)n_1n_2]^{0.5}$. However, to calculate the four quantities ν_{11}^t, ν_{22}^t, ν_{12}^t and ν_{12}^q from the system of three equations (5)–(7), knowledge of the parameters ν_0, ν_s and ν_r obtained from data processing for classical PMR is not sufficient. One way to overcome this difficulty—to determine the value of ν_{22}^t from the dependence of the amplitude of the MIS oscillations on $1/B$, which is given by the following expression [16–18]:

$$\rho_{MISO}/\rho_0 = 2(\nu_{12}^t/\nu_0)\exp[(-\pi/\omega_c) \times (\nu_{11}^q + \nu_{22}^q + 2\nu_{12}^q)]\cos(2\pi\Delta_{12}/\hbar\omega_c), \quad (8)$$

where ν_{11}^q and ν_{22}^q—single-particle relaxation rates in subbands E_1 and E_2, $\Delta_{12} = E_2 - E_1$—the value of the intersubband energy splitting, ν_0—the total transport relaxation rate. The exponent in formula (8) is the product of the Dingle factors for the individual subbands. The formula (8) is obtained from the expansion in terms of small Dingle factors up to second order [11]. The normalized amplitude of MIS oscillations in a zero reverse magnetic field according to formula (8) will be written as $\Delta\rho_{MISO}/\rho_0 = 2(\nu_{12}^t/\nu_0)$. Determining this value from the Dingle plot for the MIS oscillations allows us to find out the value of ν_{12}^t.

3. EXPERIMENTAL RESULTS AND DISCUSSION

The initial heterostructure was a 26 nm wide GaAs quantum well with short-period AlAs/GaAs superlattice barriers [12, 13]. The charge carriers in the quantum well were provided by Si δ-doping. Single Si 5-doped layers were located in AlAs/GaAs superlattice barriers on both sides of the GaAs quantum well at a distance of 29.4 nm from its boundaries. The heterostructure was grown by molecular-beam epitaxy on (001) GaAs substrate. The samples for magnetotransport measurements were Hall bridges of length L = 250 μm and width W = 50 μm equipped with top Ti/Au Schottky gates. The samples were fabricated using optical photolithography and liquid etching. The inset to Fig. 1 shows schematically the geometry of the sample.

Measurements were performed at temperatures $T = 4.2$ K in magnetic fields $B < 2$ T. The ρ_{xx} and ρ_{xy} resistances were measured in linear mode on an alternating electric current whose frequency was <1 kHz and whose amplitude did not exceed 1 μA. The Hall concentration of electrons n_H was calculated from the value of ρ_{xy} in a magnetic field of 0.5 T. The mobility μ_0 was calculated from the values of ρ_0 and n_H. The n_H and μ_0, values measured at the bridges before gate sputtering were 8.15×10^{15} m^{-2} and 119 m^2/(B s), respectively. The concentrations of charge carriers in the subbands were calculated from the oscillation period of SdH: $n_1 \approx 6.24 \times 10^{15}$ m^{-2}, $n_2 \approx 1.91 \times 10^{15}$ m^{-2}. The $E_2 - E_1$ determined from the electron concentration difference $(n_1 - n_2)$ was $\Delta_{12} \approx 15.3$ meV.

Figure 1a shows the dependencies of ρ_{xx}/p_0 on B for two gate voltages (V_g). For $V_g = 0$ in the interval 0. 1 < B < 0. 5 Tl, MIS oscillations are observed, which coexist with SdH oscillations in stronger magnetic fields. For $V_g = -2$ V, only one series of SdH oscillations is observed. Figure 1b shows the results of the Fourier analysis of the dependencies of ρ_{xx}/ρ_0 on $1/B$. Three frequencies appear in the Fourier spectrum for $V_g = 0$. Two of them correspond to the frequencies of SdH oscillations ($f_{SdH1} \approx 12.63$ T and $f_{SdH2} \approx 3.8$ T), and the third—MIS oscillations ($f_{MISO} \approx 8.83$ T). The electron concentrations in the subbands (n_j) calculated from the SchdH oscillation frequencies were: $n_1 \approx 6.11 \times 10^{15}$ m^{-2}, $n_2 \approx 1.84 \times 10^{15}$ m^{-2}. The $E_2 - E_1$ value determined from the f_{MISO} frequency was: $\Delta_{12} \approx 15$ MeV. For $V_g = -2$ V, only one ShdH oscillation frequency is observed in the Fourier spectrum, which corresponds to the electron concentration of $n_1 \approx n_H$.

Figure 2a shows the experimental dependences of n_H, n_1, n_2 and n_s on the gate voltage V_g. The dependences $n_H(V_g)$ and $n_s(V_g)$ have two characteristic intervals. In the interval V_g from 0 to −1 V, there is a weak change in n_H and n_s, and in the range from −1 to −2 V—a strong change. The nonlinear $n_s(V_g)$ dependence is due to "ejection" X of electrons from the AlAs layers adjacent to the top δ-doped layer [14]. When the gate voltage modulus $|V_g|$ is increased in the range of variation V_g from 0 to −1 V, the amplitude of the MIS oscillations drops significantly, which is due to the decreased screening of the random scattering potential of the remote donor impurity X by electrons [19]. The gate voltage between −1.2 and −2 V does not change the concentration of X-electrons in AlAs/GaAs superlattice barriers. For this reason, in this range of V_g, the dependence of $n_s(V_g)$ is close to linear [14].

The dependences of $\rho_{xx}(V_g)$, shown in Fig. 2b, show that the magnetic field significantly transforms them. In zero magnetic field, when $|V_g|$ is increased, a smooth increase in ρ_{xx} is observed due to the decrease in n_s and μ_0. The dependence of $\rho_{xx}(V_g)$ for $B = 0.5$ Tl differs significantly from $\rho_{xx}(V_g)$ in zero magnetic field only in the range of V_g from −1.2 to −1.6 V. In this range, with increasing $|V_g|$, the resistance of ρ_{xx} first increases, reaches its maximum value at $V_g = -1.4$ V, and then decreases. This behavior of $\rho_{xx}(V_g)$ was observed previously in a GaAs double quantum well and was explained by the manifestation of the classical PMR [11]. The dependence of $\rho_{xx}(V_g)$ for $B = 1$ T qualitatively differs from $\rho_{xx}(V_g)$ for $B = 0.5$ T only in the range of V_g from −1.6 to −2 V. In this range, oscillations of SdH are observed in the $\rho_{xx}(V_g)$ dependence for $B = 1$ T due to the change of concentration n1 at a fixed magnetic field value. The significant quantitative difference of $\rho_{xx}(V_g)$ in magnetic fields of 0.5 and 1 T at gate voltages of −0.9 and −1.4 V is due to the different PMR values and quantum oscillation amplitudes for these magnetic field values.

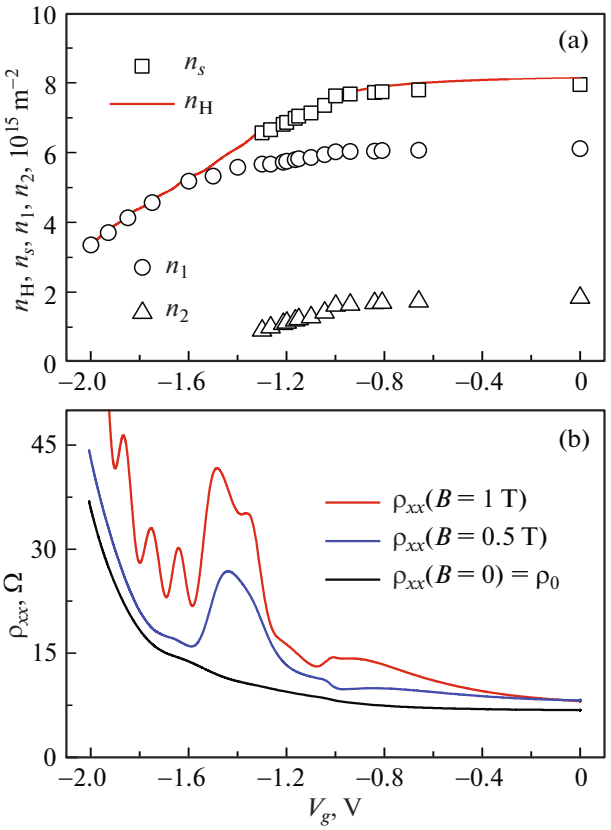

Fig. 2. (a) Experimental dependences of n_H, n_1, n_2 and n_s on V_g. (b) Experimental dependences of ρ_{xx} on V_g for different magnetic field values B.

Figure 3 shows that the theory of classical PMR in a two-subband system describes well the experimental dependences only at the initial intervals of ρ_{xx}/ρ_0 on B. This behaviour is due to the contribution to PMR of other classical and quantum mechanisms of electron scattering in two-dimensional systems [20–22]. It is evident that the deviation of the experimental depen-

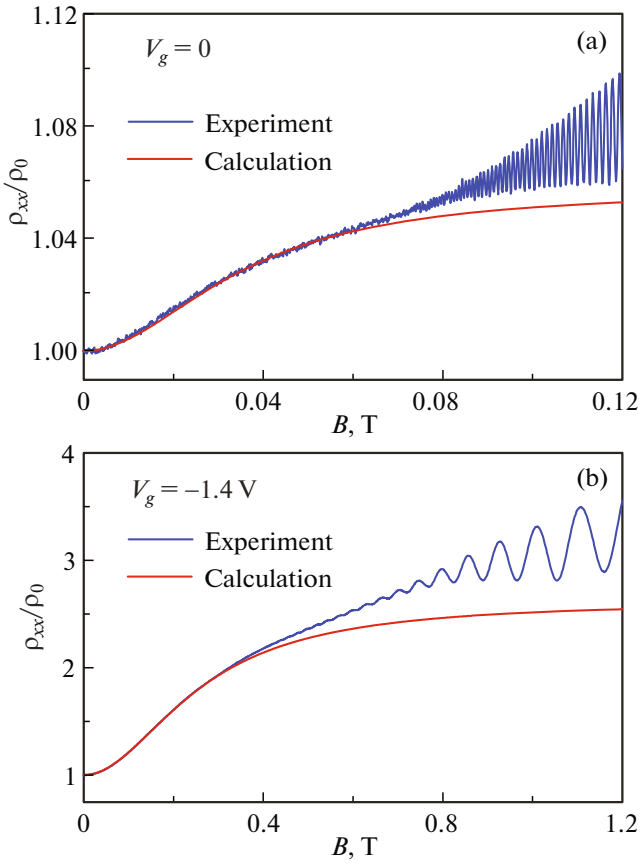

Fig. 3. Experimental dependences of ρ_{xx}/ρ_0 on B at $T = 4.2$ K for two different values of V_g and the classical PMR calculated by the formula (1). (a) $V_g = 0$: $\nu_0 = 23.12$ GHz, $\nu_s = 24.45$ GHz, $\nu_r = 92$ GHz. (b) $V_g = -1.4$ V: $\nu_0 = 27.9$ GHz, $\nu_s = 73$ GHz, $\nu_r = 670$ GHz.

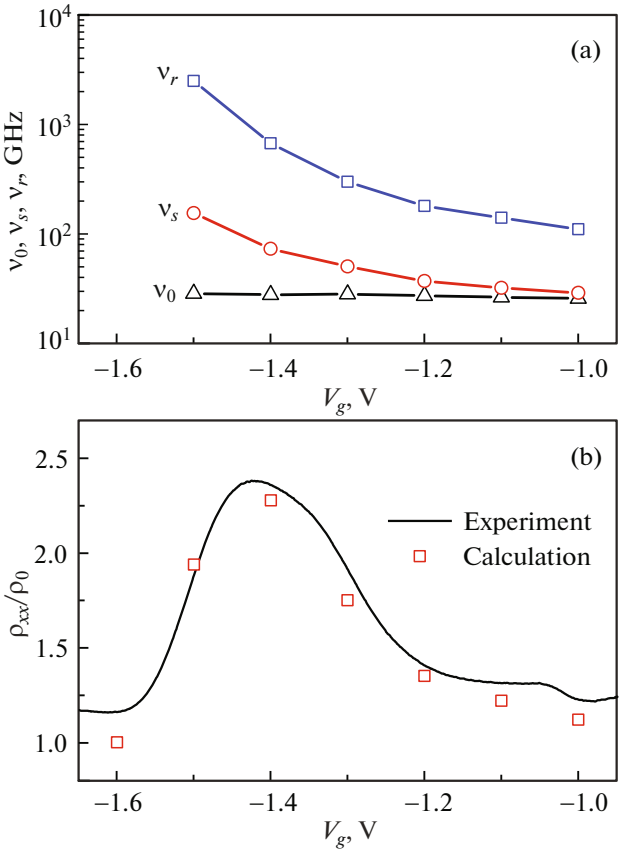

Fig. 4. (a) Dependences of ν_0, ν_s and ν_r on V_g. (b) Experimental and calculated dependence of ρ_{xx}/ρ_0 on V_g for $B = 0.5$ T.

dences from the calculated ones starts in the magnetic fields in which MIS oscillations (Fig. 3a) and SdH oscillations (Fig. 3b) occur. This behavior of ρ_{xx}/ρ_0 from B indicates that the additional contribution to the PMR has a quantum [21, 22] character. This assumption is consistent with the results of [11]. However, in our case, accounting for quantum PMR is not possible because it requires the values of ν_{11}^q and ν_{22}^q. Nevertheless, as will be seen later, fitting the calculated dependencies of ρ_{xx}/ρ_0 on B at the initial sites gives good quantitative agreement of the experiment with theory.

Figure 4a shows the dependences of ν_0, ν_s and ν_r on V_g. The values of ν_0 were determined from the experimental values of ρ_0, and ν_s and ν_r—from fitting the calculated and experimental dependences of ρ_{xx}/ρ_0 on B. The increase in these relaxation rates with increasing $|V_g|$ is primarily due to an increase in the transport relaxation rate in the second subband ν_{22}^t, since the magnitude of the Fermi vector in the second subband k_{F2} decreases most significantly with increasing $|V_g|$ compared to the relatively weakly varying magnitude of k_{F1}. The dependences of ρ_{xx}/ρ_0 on V_g, shown in Fig. 4b, demonstrate good agreement of the experimental data with the calculated ones. The observed agreement allows us to consider the fitting of the calculated and experimental dependences ρ_{xx}/ρ_0 on B at the initial parts of the curves as sufficiently correct.

Figure 5 shows the results of solving the system of equations (2)–(4) in the form of expressions (5)–(7). The dependences of $(\nu_{12}^q - \nu_{12}^t)$ and $(\nu_{11}^t + \nu_{12}^t)$ on V_g allow an unambiguous choice of physics-based solutions. As the upper subband empties, the intersubband scattering intensity decreases, which corresponds to a decrease in the relaxation rates ν_{12}^q and ν_{12}^t. Therefore, the difference $(\nu_{12}^q - \nu_{22}^t)$ should also decrease with increasing $|V_g|$ and in the limit tend to zero. At the same time the sum of $(\nu_{11}^t + \nu_{12}^t)$ must tend to ν_0. We can formally trace such a limit transition if in (3), (4) and (6) we put $\nu_{12}^q = \nu_{12}^t = 0$. Then $\nu_r \approx \nu_{22}^t$ and $\nu_0 \approx \nu_{11}^t \nu_{22}^t / \nu_r \approx \nu_{11}^t$.

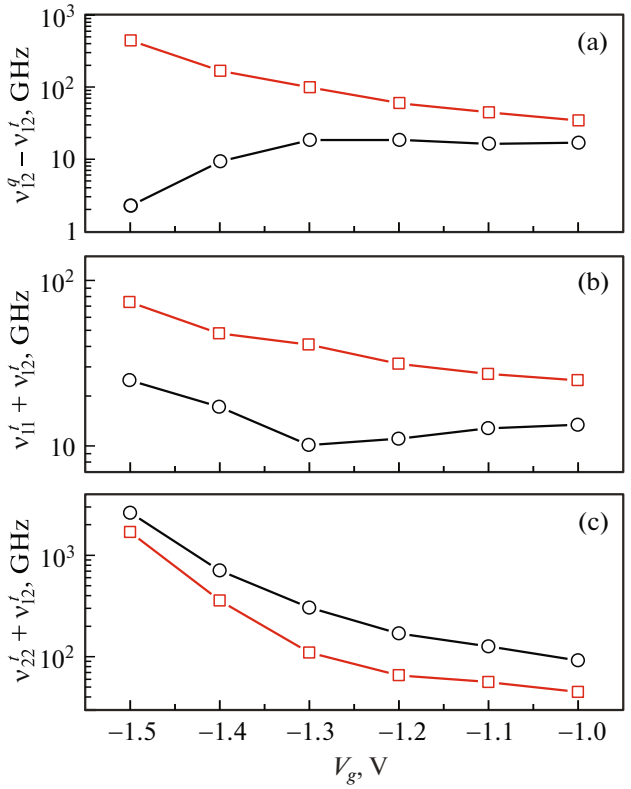

Fig. 5. The dependences of solutions (5)–(7) on V_g: (a) $(\nu_{12}^q - \nu_{12}^t)$; (b) $(\nu_{11}^t - \nu_{12}^t)$ and (c) $(\nu_{22}^t + \nu_{12}^t)$. Squares—the first set of solutions; circles—the second set of solutions.

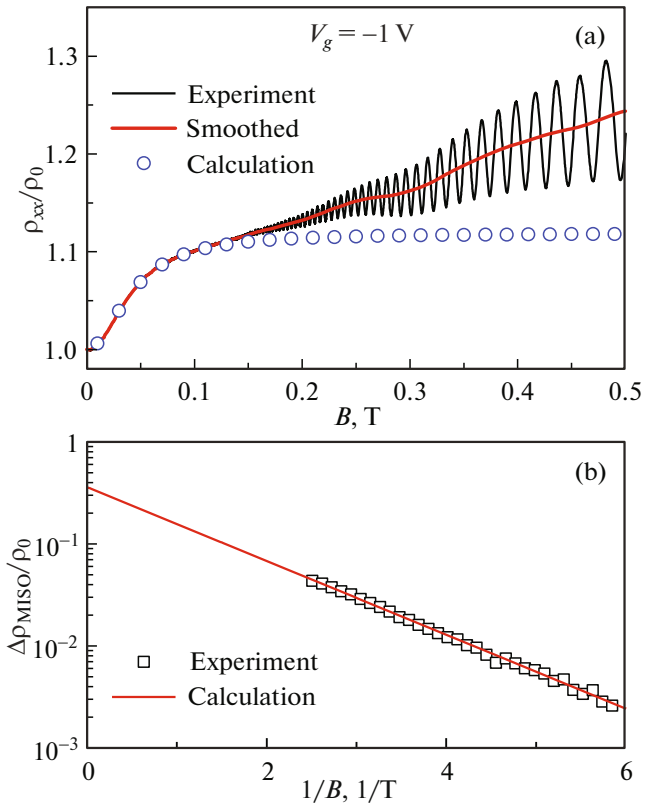

Fig. 6. (a) Experimental and smoothed dependence of ρ_{xx}/ρ_0 on B. Calculation under formula (1): ν_0 = 25.81 GHz, ν_s = 28.88 GHz, ν_r = 110 GHz. (b) Experimental dependence of $\Delta\rho_{MISO}/\rho_0$ on $1/B$. Calculation under formula $\Delta\rho_{MISO}/\rho_0 = 2(\nu_{12}^t/\nu_0)\exp[(-\pi/\omega_c)(\nu_{11}^q + \nu_{22}^q + 2\nu_{12}^q)]$: $2(\nu_{12}^t/\nu_0) = 0.36$, $(\nu_{11}^q + \nu_{22}^q + 2\nu_{12}^q) = 686$ GHz.

The above behavior of $(\nu_{12}^q - \nu_{12}^t)$ and $(\nu_{11}^t + \nu_{12}^t)$ is observed for the second set of solutions, which corresponds to the sign "–" at R in expression (5). Therefore, only this set of solutions we consider as physically justified for describing the classical PMR in the investigated single-layer two-subband system.

The experimental dependence of ρ_{xx}/ρ_0 on B, shown in Fig. 6a, shows that in the studied system for $V_g = -1$ V, in addition to PMR, MIS oscillations are well manifested. The smoothed dependence of ρ_{sm}/ρ_0 on B shows that it also exhibits magnetophononon oscillations [23, 24]. In accordance with expression (8), the dependence of the normalized MIS amplitude of $\Delta\rho_{MISO}/\rho_0$ oscillations on $1/B$ on a semi-logarithmic scale is linear. Figure 6b shows good agreement between the experimental and calculated dependences of $\Delta\rho_{MISO}/\rho_0$ on $1/B$, which allows us to determine the value of ν_{12}^t. However, correct processing of the experimental dependences of $\Delta\rho_{MISO}/\rho_0$ on $1/B$ to determine the value of ν_{12}^t is possible only in a relatively narrow interval V_g near –1 V. In the V_g band preceding this interval, the experimental dependences are not linear enough and therefore are not described by the formula (8), and in the V_g band following this interval, the amplitude of MIS oscillations is strongly suppressed [25].

The $\Delta\rho_{MISO}/\rho_0$ value found for $V_g = -1$ V in a zero reverse magnetic field is 0.36. It follows that $\nu_{12}^t \approx 0.18\nu_0 \approx 4.65$ GHz. By substituting the known values ν_0, ν_s, ν_r and ν_{12}^t into the expressions (5)–(7) for physically reasonable solutions, we can determine the transport relaxation rates of electrons in the subbands and the quantum relaxation rate for intersubband scattering, as well as the value of the ratio ν_{12}^q/ν_{12}^t at $V_g = -1$ V: $\nu_{11}^t \approx 8.8$ GHz, $\nu_{22}^t \approx 87.2$ GHz, $\nu_{12}^q \approx 21.5$ GHz, $\nu_{12}^q/\nu_{12}^t \approx 4.6$. In addition, the slope of the Dingle plot for the MIS oscillations (Fig. 6b) gives us the value of

$(\nu_{11}^q + \nu_{22}^q + 2\nu_{12}^q) = 686$ GHz, which allows us to estimate the value of the ratio

$$(\nu_{11}^q + \nu_{22}^q)/(\nu_{11}^t + \nu_{22}^t) \approx \nu_{22}^q/\nu_{22}^t \approx 6.7.$$

Such a value of ν_{22}^q/ν_{22}^t indicates that ν_{22}^q at $V_g = -1$ V is mainly determined by electron scattering on the remote impurity. Then for the quantum relaxation rate, we can write [26–28]:

$$\nu_{jj}^q \approx \nu_{jj}^{qR} = (\pi\hbar/2m)n_R^*/(k_{Fj}d_R), \quad (9)$$

where ν_{jj}^{qR}—quantum relaxation rate on remote ionized donors in j-th subband, n_R^*—effective concentration of remote ionized donors, $k_{Fj} = (2\pi n_j)^{1/2}$, $d_R = (d_S + d_{SQW}/2)$, d_S—spacer thickness, d_{SQW}—single quantum well thickness. The relaxation rate ν_{22}^q in the investigated structure at $V_g = -1$ V does not exceed 686 GHz. In this case, n_R^*, calculated by formula (9), does not exceed 10^{15} m^{-2}.

For a relatively dense ($n > 10^{15}$ m^{-2}) high-mobility 2D electron gas at low temperatures, the transport relaxation rate is determined by two main scattering mechanisms: scattering on distant charged impurities and on the background impurity. Therefore, the transport relaxation rate in the jth subband is expressed as

$$\nu_{jj}^t = \nu_{jj}^{tR} + \nu_{jj}^{tB}, \quad (10)$$

where ν_{jj}^{tR}—transport relaxation rate on remote ionized donors, and ν_{jj}^{tB}—transport relaxation rate on charged background impurities. The intra-subband transport relaxation rate on remote ionized donors in the jth subband is given by the following relation [26–28]:

$$\nu_{jj}^{tR} = (\pi\hbar/8m)n_R^*/(k_{Fj}d_R)^3. \quad (11)$$

For a concentration value of $n_R^* = 10^{15}$ m^{-2}, the corresponding value of ν_{22}^{tR}, calculated by formula (11), is 9.8 GHz. The large difference between the $\nu_{22}^{tR} \approx 9.8$ GHz and $\nu_{22}^t \approx 87.2$ GHz values indicates that ν_{22}^t, unlike ν_{22}^q, is not determined by scattering on the random potential of distant ionized donors alone. When $V_g = -1$ V, the value of $\nu_{22}^t/\nu_{11}^t \approx 9.9$ is comparable to that of $(n_1/n_2)^{1.5} \approx 8.2$. This fact allows us to consider that ν_{11}^t and ν_{22}^t are determined by electron scattering on two types of random potential—remote dopant impurity and background impurity, having the same dependence of transport relaxation rates on n_j.

The intrasubband electron transport relaxation rate for scattering on charged background impurities with volume concentration n_B can be expressed by the following relation [26–28]:

$$\nu_{jj}^{tB} \approx (m/2\pi\hbar^3)(e^2/2\varepsilon_0\varepsilon)^2 n_B/k_{Fj}^3, \quad (12)$$

where ε_0—electrical constant, ε—relative dielectric constant of the quantum well. At $V_g = -1$ V the value of $\nu_{22}^{tB} = \nu_{22}^t - \nu_{22}^{tR} \approx 77.4$ GHz. The concentration corresponding to this value n_B, calculated by formula (12), is 7×10^{20} m^{-3}. Note that the n_B value characterizes the quality of the structure and, unlike n_R^*, is independent of the gate voltage.

For the investigated two-subband system at $V_g = -1.5$ V, the results of solving the system of equations (2)–(4), represented by the expressions (5)–(7), allow the electron groups in the first and second subbands to be considered independent, since for this gate voltage ν_{12}^t is significantly smaller than ν_{11}^t and ν_{22}^t. Expressions (6) and (7) give the following values for the transport relaxation rates ν_{11}^t and ν_{22}^t for $V_g = -1.5$ V: $\nu_{11}^t \approx 25$ GHz and $\nu_{22}^t \approx 2626$ GHz. The obtained values of ν_{11}^t and ν_{22}^t are close to the values of $\nu_0 \approx 28.6$ GHz and $\nu_r \approx 2500$ GHz, respectively, as they should be for two independent groups of charge carriers under condition $n_1 \gg n_2$. The magnitude of the $\nu_{22}^t/\nu_{11}^t \approx 100.5$ ratio is approximately the same as the magnitude of the ratio $(n_1/n_2)^{1.5} \approx 82.8$. Thus, it can be concluded that in the studied system at $V_g = -1.5$ V, as well as at $V_g = -1$ V, the relaxation rates ν_{11}^t and ν_{22}^t are determined by scattering on two types of random potential—remote alloying impurity and background impurity. The transport relaxation rate of ν_{11}^{tB} at $V_g = -1.5$ V is 12 GHz. In this case, $\nu_{11}^{tR} = \nu_{11}^{tB} \approx 13$ GHz.

The effective concentration of n_R^* at $V_g = -1.5$ V for $\nu_{11}^{tR} \approx 13$ GHz is 9×10^{15} m^{-2}. The resulting n_R^* at $V_g = -1.5$ V is about an order of magnitude larger than the n_R^* at $V_g = -1$ V. This means that when $V_g = -1$ V the value of n_R^* has not yet reached its maximum value, which is practically independent of V_g. However, the dependence of $n_s(V_g)$, which is close to linear in the range of V_g from -1.2 to -2 V, allows us to consider that in this range of gate voltages n_R^* takes its maximum value, which is 9×10^{15} m^{-2}. The results show

that in the interval V_g from -1.2 to -2 V the two-subband electron transport in the investigated structure is determined by scattering on the remote dopant impurity with the effective concentration of charged donors $n_R^* \approx 9 \times 10^{15}$ m^{-2} and charged background impurity with the concentration $n_B \approx 7 \times 10^{20}$ m^{-3}.

4. CONCLUSIONS

Based on a single GaAs quantum well with symmetric modulated superlattice doping, a high-mobility electronic system with two filled subbands E_1 and E_2 of dimensional quantization has been realized. The transition from two-subband to single-subband transport has been studied in a single-layer two-subband system by varying the magnitude of the negative voltage V_g on the Schottky gate to such a quantum well.

The dependence of the total electron concentration $n_s = n_1 + n_2$ in a single GaAs-quantum well with AlAs/GaAs superlattice barriers on the gate voltage $n_s(V_g)$ is found to have two characteristic regions with different values of the average slope. The observed behavior is consistent with the results of [14] and is due to the fact that changing the voltage V_g in the range from 0 to -1.2 V changes not only n_s in the single GaAs quantum well, but also the concentration of X-electrons in the upper barrier to it, but in the range from -1.2 to -2 V changes only n_s.

It is also found that when V_g is varied from 0 to -1.2 V, the amplitude of the MIS oscillations decreases. This behavior is explained by an increase in the effective concentration of remote ionized donors n_R^* due to a decrease in the concentration of X-electrons in the upper barrier [19] and a corresponding increase in the quantum relaxation rates in the subbands ν_{jj}^{qR}.

It is found that in the single-layer two-subband system, as well as in the bilayer [11] system, the classical PMR observed when a negative voltage is applied to the Schottky gate first rises and then falls. This behavior is explained by the depletion of the upper subband E_2 and is consistent with the theory of classical PMR, which accounts for the role of intersubband scattering in two-subband magnetotransport [9, 11]. It is shown that the joint analysis of classical PMR and MMP oscillation amplitude provides an opportunity to estimate the concentration of charged background impurities n_B and, accordingly, to evaluate the quality of high-mobility two-subband heterostructures.

ACKNOWLEDGMENTS

The authors thank G.M. Minkov for fruitful discussion of the work results.

FUNDING

The study was supported by the Russian Science Foundation (no. RFN-22-22-00726, https://rscf.ru/project/22-22-00726/).

CONFLICT OF INTEREST

The authors of this work declare that they have no conflicts of interest.

REFERENCES

1. H. Stormer, R. Dingle, A. Gossard, W. Wiegmann, M. Sturge. Solid State Commun., **29**, 705 (1979).
2. H. Stormer, A. Gossard, W. Wiegmann. Solid State Commun., **41**, 707 (1982).
3. H. van Houten, J. G. Williamson, M. E. I. Broekaart, C. T. Foxon, J. J. Harris. Phys. Rev. B, **37**, 2756 (1988).
4. T. P. Smith III, F. F. Fang. Phys. Rev. B, **37**, 4303 (1988).
5. P. T. Coleridge. Semicond. Sci. Technol., **5**, 961 (1990).
6. D. R. Leadley, R. Fletcher, R. J. Nicholas, F. Tao, C. T. Foxon, J. J. Harris. Phys. Rev. B, **46**, 12439 (1992).
7. S. Mori, T. Ando. Phys. Rev. B, **19**, 6433 (1979).
8. V. M. Polyanovskii. Fiz. Tekh. Poluprov., **22**, 2230 (1988). [Sov. Phys. Semicond., **22**, 1408 (1988)].
9. E. Zaremba. Phys. Rev. B, **45**, 14143 (1992).
10. R. Fletcher, M. Tsaousidou, T. Smith, P. T. Coleridge, Z. R. Wasilewski, Y. Feng. Phys. Rev. B, **71**, 155310 (2005).
11. N. C. Mamani, G. M. Gusev, E. C. F. da Silva, O. E. Raichev, A. A. Quivy, A. K. Bakarov. Phys. Rev. B, **80**, 085304 (2009).
12. K.-J. Friedland, R. Hey, H. Kostial, R. Klann, K. Ploog. Phys. Rev. Lett., **77**, 4616 (1996).
13. A. V. Goran, A. A. Bykov, A. I. Toropov, S. A. Vitkalov. Phys. Rev. B, **80**, 193305 (2009).
14. A. A. Bykov, I. S. Strygin, A. V. Goran, D. V. Nomokonov, A. K. Bakarov. JETP Lett., **112**, 437 (2020).
15. A. A. Bykov, D. V. Nomokonov, A. V. Goran, I. S. Strygin, I. V. Marchishin, A. K. Bakarov. Semiconductors, **57**, 180 (2023). [FTP, **57**, 181 (2023). (in Russian).]
16. M. E. Raikh, T. V. Shahbazyan. Phys. Rev. B, **49**, 5531 (1994).
17. N. S. Averkiev, L. E. Golub, S. A. Tarasenko, M. Willander. J. Phys.: Condens. Matter, **13**, 2517 (2001).
18. O. E. Raichev. Phys. Rev. B, **78**, 125304 (2008).
19. M. Sammon, M. A. Zudov, B. I. Shklovskii. Phys. Rev. Mater., **2**, 064604 (2018).

20. D. G. Polyakov, F. Evers, A. D. Mirlin, P. Wolfle. Phys. Rev. B, **64**, 205306 (2001).
21. M. G. Vavilov, I. L. Aleiner. Phys. Rev. B, **69**, 035303 (2004).
22. S. Dietrich, S. Vitkalov, D. V. Dmitriev, A. A. Bykov. Phys. Rev. B, **85**, 115312 (2012).
23. A. A. Bykov, A. V. Goran, S. A. Vitkalov. Phys. Rev. B, **81**, 155322 (2010).
24. O. E. Raichev. Phys. Rev. B, **81**, 195301 (2010).
25. A. A. Bykov, D. V. Nomokonov, A. V. Goran, I. S. Strygin, A. K. Bakarov, S. Abedi, S. A. Vitkalov. JETP Lett., **114**, 423 (2021).
26. A. Gold. Phys. Rev. B, **38**, 10798 (1988).
27. I. A. Dmitriev, A. D. Mirlin, D. G. Polyakov, M. A. Zudov. Rev. Mod. Phys., **84**, 1709 (2012).
28. J. H. Davies. *The Physics of Low Dimensional Semiconductors* (Cambridge University Press, N.Y., 1998).

Translated by Ego Translating